Schwinger-Keldysh approach to disordered and interacting electron systems: Derivation of Finkelstein's renormalization-group equations

Claudio Chamon
Department of Physics, University of Illinois at Urbana-Champaign, Urbana, Illinois 61801-3080
and Department of Physics, Boston University, Boston, Massachusetts 02215

Andreas W. W. Ludwig
Physics Department, University of California, Santa Barbara, California 93106-4030
and Institute for Theoretical Physics, University of California, Santa Barbara, California 93106-4030

Chetan Nayak
Institute for Theoretical Physics, University of California, Santa Barbara, California 93106-4030
and Physics Department, University of California, Los Angeles California 90095-1547
(Received 4 November 1998)

We develop a dynamical approach based on the Schwinger-Keldysh formalism to derive a field-theoretic description of disordered and interacting electron systems. Within this formalism we calculate the perturbative renormalization-group (RG) equations for interacting electrons expanded around a diffusive Fermi liquid fixed point, as obtained originally by Finkelstein (Zh. Éksp. Teor. Fiz. **84**, 168 (1983) [Sov. Phys. JETP **57**, 97 (1983)]) using replicas. The major simplifying feature of this approach, as compared to Finkelstein's, is that instead of $N\to 0$ replicas, we only need to consider $N=2$ species. We compare the dynamical Schwinger-Keldysh approach and the replica methods, and we present a simple and pedagogical RG procedure to obtain Finkelstein's RG equations. [S0163-1829(99)03427-X]

I. INTRODUCTION

Since the original idea of an impurity driven metal-insulator transition (MIT) was put forward by Anderson,[1] a substantial amount of work has been carried out to understand this problem in the language of phase transitions and of the renormalization group (RG).[2–4] Simple scaling arguments were made for the case of noninteracting electrons. It was demonstrated that there would always be a metal-to-insulator transition in three dimensions as a function of the disorder strength, whereas in one and two dimensions even the weakest amount of disorder would make the system an insulator at zero temperature.[4] The lower critical dimension for the MIT is $d=2$ for the noninteracting electron problem, and $\epsilon=d-2$ expansions have been carried out to determine the critical exponents characterizing the phase transition.[3]

These scaling ideas were extended to include the effects of electron-electron interactions by Finkelstein,[5] and later by Castellani *et al.*,[6] who obtained RG equations for the conductance, as well as the singlet and triplet interaction coupling constants, starting with a diffusive Fermi-liquid fixed point (for a review, see Ref. 7). This seminal work defined a field-theoretical language to study the simultaneous presence of interactions and disorder. Unfortunately, this approach suffered from being inconclusive — since the coupled renormalization-group equations flow to strong coupling, away from the perturbative starting point of a diffusive Fermi-liquid state — and technically quite involved. A recent discussion of Finkelstein's replica theory can be found in Ref. 8.

The recent experimental discovery by Kravchenko and co-workers[9] of a MIT in a two-dimensional Si-MOSFET (metal-organic semiconductor field-effect transistor), and the subsequent discovery of such a transition in other two-dimensional[10–12] electron-gas systems, has rekindled interest in sharpening our understanding of the combined effects of disorder and interactions. In this paper we will rederive the RG equations for all marginal perturbations of the diffusive Fermi-liquid fixed point (there are no relevant perturbations). We will do so using the dynamical Schwinger-Keldysh approach. Our results agree with those obtained using the replica method[5] and disorder-averaged perturbation theory.[6] As we will show, the Schwinger-Keldysh and replica approaches to studying the diffusive Fermi liquid exhibit very similar structures. It is important to note that, in the replica solution, there are no subtleties involved in the $N\to 0$ replica limit at the perturbative level, which reflects the fact that that there is no replica symmetry breaking in the diffusive Fermi liquid state. This is the underlying reason why the Schwinger-Keldysh and replica solutions, as we will see, look very much alike, with the dynamical thermal indices for time-ordered and anti-time-ordered fields behaving as simple bookkeeping devices, just as in the replica solution. On the other hand, glassy systems which exhibit replica symmetry breaking, such as the recently proposed Wigner glass phase,[13,14] should be rather different and more interesting. We will explore these directions in the future. In the present paper, we will limit ourselves to the study of the diffusive Fermi liquid, which we present below.

We present the Schwinger-Keldysh approach for disordered and interacting electronic systems in Sec. II, where we show that instead of $N\to 0$ replicas, we only need to consider $N=2$ species of fields. Using this dynamic approach, in Sec. III we derive a nonlinear σ model for interacting diffusion

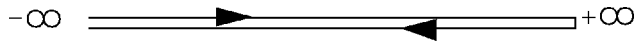

FIG. 1. Keldysh contour, going from $-\infty$ to ∞ and back to $-\infty$.

modes in the Schwinger-Keldysh formalism. For simplicity, we restrict attention to the ''unitary'' case considered in Finkelstein's original paper:[5] we assume that the electrons interact through a short-range interaction, and that they are in a magnetic field which affects their orbital motion, but that the Zeeman coupling vanishes (this situation might be realizable in GaAs-$Al_xGa_{1-x}As$ systems). By straightforward extension of the methods used here, we can also treat the more interesting, but more complicated, ''orthogonal'' case in which the magnetic field is turned off. In a similar vein, we avoid the straightforward but more involved extension to long-range Coulomb interactions. This would include applications of our approach to the quantum Hall plateau transitions. We emphasize the similarities and differences with the replicated σ model. In Sec. IV, we find the diffusive saddle point and bring the σ model into a form which is convenient for perturbation theory about this saddle point. This form is used to derive the Feynman rules, given in Sec. V, which are needed for one-loop perturbative calculations. In Sec. VI, we use these Feynman rules to discuss the one-loop renormalization of this σ model. One of our main purposes here is pedagogy, so we discuss the diagrammatics in detail, paying attention to the symmetry factors and minus signs which prove to be crucial in determining the physics of the model. As we show, the apparent complexity — due to the large number of diagrams — can be offset by a systematic enumeration. Finally, in Secs. VII and VIII, we discuss the resulting RG equations, a constraint on them following from the Ward identity for charge conservation, and their physics.

II. DYNAMICAL SCHWINGER-KELDYSH APPROACH TO DISORDERED AND INTERACTING ELECTRONS

In the Schwinger-Keldysh — or closed-time path — formalism,[15–17] a functional integral (see also the formulation by Feynman and Vernon[18]) is constructed for the time evolution of the vacuum state from $t=-\infty$ to $t=\infty$ and back to $t=-\infty$ (the Keldysh contour, shown in Fig. 1, is just one possible path for this evolution). Such evolution of the vacuum brings it back to the initial state, and therefore the vacuum-to-vacuum overlap (or vacuum persistence Z) in the closed-path formalism is 1. Consequently, the functional integral is automatically normalized to $Z=1$ for any realization of the disorder potential, so disorder-averaged correlation functions can be calculated directly from the disorder-averaged functional integral. The price which must be paid is the doubling of the number of the fields in the theory; the second copy of each field propagates backwards in time.

The application of dynamical approaches, such as the Schwinger-Keldysh formalism, to disordered systems was previously proposed. At the classical level, Martin, Siggia, and Rose[19] used a dynamical approach and explored the independence of the classical generating functional on the disorder. Sompolinsky[20] used this formalism to study the mean-field theory for the spin-glass problem. Quantum versions of the idea of using dynamics to enforce $Z=1$ were proposed

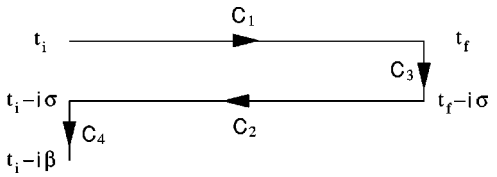

FIG. 2. Real-time contour separated into four parts that factorize into separate contributions: $C_1 \cup C_2$ and $C_3 \cup C_4$.

by Schuster and Vieira[21] and Kree.[22] However, these proposals were never stated in a language suitable for calculations in disordered systems. A concrete formulation was put forward by Horbach and Schön,[23] who developed a time-path formulation for disordered noninteracting electrons. Recently, Cugliandolo and Lozano[24] proposed a closed-time path formalism for quantum spin glasses. In work complementary to ours, Andreev and Kamenev[25] used the Schwinger-Keldysh formalism to address the issue of gauge invariance in disordered interacting electron systems. They discussed the single-particle density of states — which we do not — but did not derive the full set of coupled RG equations — which we do, following Finkelstein.

Here we apply the closed-time path formulation, and cast it in a language appropriate to consider the effect of interactions. We give an extended discussion of the method in Ref. 26, where we discuss, in addition to systems with a natural quantum dynamics, a nontrivial extension of the method to systems with no natural quantum or classical dynamics, such as disordered, interacting statistical field theories. Below we give a short summary of the method.

The Keldysh contour in Fig. 1 is just one example of a possible contour for which we can achieve our desired objective, namely, the absence of a denominator in the correlation functions (i.e., $Z=1$). Here we will discuss a more general class of contours originally devised for the study of field theories at finite temperatures.[27–29] These formulations are carried out in real time, and their objective was to circumvent pitfalls from the strong assumptions about analytical continuation of imaginary-time (such as Matsubara's) formulations.

At finite temperature, the contour of Fig. 1 is replaced by a contour running from $t=-\infty$ to $t=\infty$ and thence to $t=-\infty-i\beta$. A contour of this type is displayed in Fig. 2. For such a contour, there is an important factorization property,[26] shown in Ref. 29, for the contributions from each piece of the contour to the functional integral Z:

$$Z=Z^{C_1\cup C_2}Z^{C_3\cup C_4}. \tag{1}$$

Only C_1 and C_2 are important in obtaining physical correlation functions.[30] As a consequence of the factorization property, we can obtain these correlation functions from $Z^{C_1\cup C_2}$ which satisfies the normalization property

$$Z^{C_1\cup C_2}=1. \tag{2}$$

Hence, even at finite-temperature, we can work with a partition function normalized to 1. Denoting the fields on the upper (C_1) and the lower (C_2) pieces of the countour by

$$\phi_1(t)=\phi(t), \quad \phi_2(t)=\phi(t-i\sigma) \quad (t \text{ real}) \tag{3}$$

one defines a matrix propagator

$$\langle T_c[\phi_a(t,x)\phi_b^\dagger(t',x')]\rangle = -i\Delta_{ab}(t-t',x-x'), \quad (4)$$

where T_c denotes ordering of fields according their position along the contour of Fig. 2. The particular choice $\sigma=\beta/2$ makes the form of the propagators especially simple. Let ϕ denote a complex field, bosonic or fermionic. The propagator $i\Delta^{ab}$ can be written in terms of the zero-temperature propagator $i\Delta_0^{ab}$ as

$$i\Delta(\omega,k) = u(\omega) i\Delta_0(\omega,k) u^\dagger(\omega), \quad (5)$$

where

$$i\Delta_0(\omega,k) = \begin{pmatrix} iG_0(\omega,k) & 0 \\ 0 & -iG_0^*(\omega,k) \end{pmatrix}, \quad (6)$$

with $iG_0(\omega,k)$ the usual time-ordered propagator,

$$iG_0(t-t',x-x') = \langle T[\phi(t,x)\phi^\dagger(t',x')]\rangle, \quad (7)$$

and $-iG_0^*(\omega,k)$, consequently, the anti-time-ordered one

$$-iG_0^*(t-t',x-x') = \{\langle T[\phi(t,x)\phi^\dagger(t',x')]\rangle\}^* = \langle \overline{T}[\phi(t',x')\phi^\dagger(t,x)]\rangle. \quad (8)$$

The matrix u contains the information about the temperature. For bosonic fields, this matrix is given by

$$u(\omega) = u_B(\omega) = \begin{pmatrix} \cosh\Delta\theta_\omega & \sinh\Delta\theta_\omega \\ \sinh\Delta\theta_\omega & \cosh\Delta\theta_\omega \end{pmatrix} \quad \text{where} \quad \Delta\theta_\omega = \theta_\omega^T - \theta_\omega^{T=0} \quad \text{and} \quad \cosh^2\theta_\omega^T = \frac{1}{1-e^{-\omega/T}}. \quad (9)$$

For a fermion field, the matrix is altered to account for the fermionic statistics, and we have

$$u(\omega) = u_F(\omega) = \begin{pmatrix} \cos\Delta\theta_\omega & \sin\Delta\theta_\omega \\ -\sin\Delta\theta_\omega & \cos\Delta\theta_\omega \end{pmatrix} \quad \text{where} \quad \Delta\theta_\omega = \theta_\omega^T - \theta_\omega^{T=0} \quad \text{and} \quad \cos^2\theta_\omega^T = \frac{1}{1+e^{-(\omega-\mu)/T}}. \quad (10)$$

Notice that at zero temperature $u_{B,F}=\mathbf{1}$.

All correlation functions in a theory with propagator Δ_{ab} and interaction $\mathcal{L}[\phi,\phi^*]$ are obtained using the following functional integral over two fields $\phi_{1,2}$:

$$Z = \int D\phi_1 D\phi_2 \exp\left[i\int dt\, d^dx \left(\frac{1}{2}\phi_a^*[\Delta^{-1}]^{ab}\phi_b + \mathcal{L}_I[\phi_1,\phi_1^*] - \mathcal{L}_I[\phi_2,\phi_2^*] \right)\right], \quad (11)$$

where all time integrals are to be done from $-\infty$ to ∞. This gives rise to a crucial relative sign in how the interaction comes in for the forward-propagating field ϕ_1 and the backward-propagating field ϕ_2.

III. NONLINEAR SIGMA MODEL WITHIN THE SCHWINGER-KELDYSH FORMALISM

We start by deriving a nonlinear σ model in the language of the dynamical Schwinger-Keldysh formalism. The steps are quite similar to the derivation in the replica formulation. As shown above, we formulate the problem in terms of a real-time path integral

$$Z = \int D\psi^\dagger D\psi\, e^{iS[\psi^\dagger,\psi]} \quad (12)$$

for a fermionic field

$$\psi = \begin{pmatrix} \psi_1 \\ \psi_2 \end{pmatrix}$$

comprised of two components ψ_i labeled by the thermal indices $i=1$ and 2 (in addition to other indices such as spin). The index $i=1$ corresponds to time-ordered fields, and $i=2$ to anti-time-ordered ones.

A. Free action

The free part of the action for these fermions can be written as

$$S_0[\psi^\dagger,\psi] = \int d^dx \int \frac{d\omega}{2\pi} \psi^\dagger(x,\omega) u_F(\omega)\sigma_3 \times \begin{bmatrix} \omega + \dfrac{\nabla^2}{2m} + \epsilon_F + i\eta\,\mathrm{sgn}\,\omega & 0 \\ 0 & \omega + \dfrac{\nabla^2}{2m} + \epsilon_F - i\eta\,\mathrm{sgn}\,\omega \end{bmatrix} \times u_F^\dagger(\omega)\psi(x,\omega), \quad (13)$$

from which we obtain the free matrix propagator

$$\widehat{\psi\psi}^\dagger = i\Delta(\omega,k) = u_F(\omega) i\Delta_0(\omega,k) u_F^\dagger(\omega), \quad (14)$$

where

$$i\Delta_0(\omega,k) = \begin{bmatrix} iG_0(\omega,k) & 0 \\ 0 & -iG_0^*(\omega,k) \end{bmatrix}, \quad (15)$$

and iG_0 is the time-ordered propagator

$$iG_0(\omega,k) = \frac{i}{\omega - \dfrac{k^2}{2m} + \epsilon_F + i\eta\,\mathrm{sgn}\,\omega}.$$

Notice that the anti-time-ordered propagator is the adjoint of iG_0. The matrix $u_F(\omega)$ containing the temperature dependence was defined above. In particular, $u_F(\omega)=\mathbf{1}_{\text{thermal}}$ at $T=0$. In this case we have

$$S_0[\psi^\dagger,\psi]=\int d^dx\int\frac{d\omega}{2\pi}\overline{\psi}(x,\omega)\times\left[\left(\omega+\frac{\nabla^2}{2m}+\epsilon_F\right)\mathbf{1}+i\eta\sigma_3 f\,\mathrm{sgn}\,\omega\right]\psi(x,\omega), \tag{16}$$

where in the last line we defined $\overline{\psi}=\psi^\dagger\sigma_3$.

B. Disorder term

The static disorder contribution to the action is

$$S_V[\psi^\dagger,\psi]=\int d^dx\int\frac{d\omega}{2\pi}V(x)\psi^\dagger(x,\omega)\sigma_3\psi(x,\omega). \tag{17}$$

Notice that any interaction term entering the action has the following properties.

(1) It does not mix the two fields $\psi_{1,2}$. There will be mixing after disorder averaging, but not before.

(2) The contributions from the two thermal components $i=1$ and 2 enter with opposite signs (thus the σ_3) due to the negative sign for the time integration along the anti-time-ordered branch.

The disorder potential is assumed to be Gaussian distributed according to

$$P[V(x)]\propto e^{(-1/2u)\int dx\,V^2(x)}. \tag{18}$$

We then integrate out the disorder, using the fact that the Schwinger-Keldysh formulation cancels the denominator problem

$$e^{iS_{\text{rand}}[\psi^\dagger,\psi]}=\int DV\,P[V]e^{iS_V[\psi^\dagger,\psi]}, \tag{19}$$

thus generating a four-fermion term

$$\begin{aligned}S_{\text{rand}}[\psi^\dagger,\psi]&=i\frac{u}{2}\int d^dx\int\frac{d\omega}{2\pi}\frac{d\omega'}{2\pi}\psi^\dagger(x,\omega)\sigma_3\psi(x,\omega)\psi^\dagger(x,\omega')\sigma_3\psi(x,\omega')\\&=i\frac{u}{2}\int d^dx\int\frac{d\omega}{2\pi}\frac{d\omega'}{2\pi}\overline{\psi}(x,\omega)\psi(x,\omega)\overline{\psi}(x,\omega')\psi(x,\omega').\end{aligned} \tag{20}$$

Let us now introduce the Hubbard-Stratonovich matrix field Q that decouples the four fermions (the matrix Q is chosen to be Hermitian). We will choose the decoupling in the diffusive particle-hole channel. As in the case of the original diffusive Fermi liquid study by Finkelstein, here we will not consider the Cooperon contributions. We have

$$e^{iS_{\text{rand}}[\overline{\psi},\psi]}=\int DQ\,e^{(-1/2u)\int d^dx\,\mathrm{tr}\,Q^2}e^{iS_{\text{HS}}[Q,\overline{\psi},\psi]} \tag{21}$$

where

$$S_{\text{HS}}[Q,\overline{\psi},\psi]=i\int d^dx\int\frac{d\omega}{2\pi}\frac{d\omega'}{2\pi}\overline{\psi}(x,\omega)Q_{\omega\omega'}(x)\psi(x,\omega'). \tag{22}$$

The matrix Q has indices in three separate spaces, i.e., it is assembled as a direct product in energy, thermal, and spin spaces:

$$Q^{ij,\alpha\beta}_{\omega\omega'}=[Q^{ji,\beta\alpha}_{\omega'\omega}]^*\quad\text{Hermitian.}$$

Thus the trace of Q^2 corresponds to

$$\mathrm{tr}\,Q^2=\int\frac{d\omega}{2\pi}\frac{d\omega'}{2\pi}\sum_{i,j=1}^{2}\sum_{\alpha,\beta=1}^{2}Q^{ij,\alpha\beta}_{\omega\omega'}Q^{ji,\beta\alpha}_{\omega'\omega}.$$

When we write $Q_{\omega\omega'}$ we mean a matrix whose elements are matrices in thermal $(i,j=1,2)$ and spin spaces $(\alpha,\beta=1,2)$.

We can then write an expression for Z as a functional integral over $\overline{\psi},\psi$ and Q:

$$Z=\int DQ\int D\overline{\psi}D\psi e^{(-1/2u)\int d^dx\,\mathrm{tr}Q^2}e^{iS_0[\overline{\psi},\psi]}e^{iS_{\text{HS}}[Q,\overline{\psi},\psi]}, \tag{23}$$

where, writing S_0 and S_{HS} explicitly in terms of sums over the energy, thermal, and spin indices

$$\begin{aligned}S_0+S_{\text{HS}}=\int d^dx\int\frac{d\omega}{2\pi}\frac{d\omega'}{2\pi}\sum_{ij,\alpha\beta}\overline{\psi}_{i,\alpha}(x,\omega)&\times\left\{\left[\left(\omega+\frac{\nabla^2}{2m}+\epsilon_F\right)\delta_{ij}+i\eta\sigma_3^{ij}\,\mathrm{sgn}\,\omega\right]\right.\\&\left.\times\delta_{\alpha\beta}\delta_{\omega\omega'}+iQ^{ij,\alpha\beta}_{\omega\omega'}(x)\right\}\psi_{j,\beta}(x,\omega').\end{aligned} \tag{24}$$

Upon integrating out the fermions we obtain an effective theory for the matrix Q field,

$$\begin{aligned}Z=\int DQ\,e^{(-1/2u)\int d^dx\,\mathrm{tr}\,Q^2}&\times\exp\left\{\int d^dx\,\mathrm{tr}\ln\left[-i\Omega-i\left(\frac{\nabla^2}{2m}+\epsilon_F\right)\mathbf{1}\right.\right.\\&\left.\left.+\eta\Lambda+Q(x)\right]\right\},\end{aligned} \tag{25}$$

where we introduced Ω and Λ as matrices in the energy $\otimes$ thermal $\otimes$ spin spaces:

$$\Omega^{ij,\alpha\beta}_{\omega\omega'} = \omega\,\delta_{\omega\omega'}\delta_{ij}\delta_{\alpha\beta} \tag{26}$$

and

$$\Lambda^{ij,\alpha\beta}_{\omega\omega'} = \mathrm{sgn}\,\omega\,\delta_{\omega\omega'}\sigma_3^{ij}\delta_{\alpha\beta}$$

or

$$\Lambda = \underbrace{\Sigma_3}_{\text{Energy}} \otimes \underbrace{\sigma_3}_{\text{Thermal}} \otimes \underbrace{\mathbf{1}}_{\text{Spin}}, \tag{27}$$

with Σ_3 defined as a matrix in energy space that is diagonal and whose entries are $+1$ for positive energies and -1 for negative ones.

Equation (25) is the nonlinear σ model for a noninteracting system. The information necessary to dispose of disconnected loops generated by the disorder average is encoded in the matrix structure for Ω and Λ. This structure ensures that we can work with only two indices, $i,j=1,2$, instead of N replicas with $N\to 0$ at the end. Notice, however, that very much like in the replicated sigma model, the disorder connects Q components sitting on different indices. Next, we will add the contributions due to interactions.

C. Interaction term

Let us consider the case of short-range interactions, in the singlet and triplet channels:

$$S_{\rm int} = S_1 + S_2$$

where

$$S_1[\psi^\dagger,\psi] = \pi\Gamma_1 \int d^dx \int \frac{d\omega}{2\pi}\frac{d\omega'}{2\pi}\frac{d\epsilon}{2\pi} \sum_{ij,\alpha\beta} \psi^\dagger_{i,\alpha}(x,\omega)\psi_{i,\beta}(x,\omega+\epsilon)\sigma_3^{ij}\psi^\dagger_{j,\beta}(x,\omega'+\epsilon)\psi_{j,\alpha}(x,\omega')$$

$$= \pi\Gamma_1 \int d^dx \int \frac{d\omega}{2\pi}\frac{d\omega'}{2\pi}\frac{d\epsilon}{2\pi} \sum_{ij,\alpha\beta} \overline{\psi}_{i,\alpha}(x,\omega)\psi_{i,\beta}(x,\omega+\epsilon)\sigma_3^{ij}\overline{\psi}_{j,\beta}(x,\omega'+\epsilon)\psi_{j,\alpha}(x,\omega') \tag{28}$$

and

$$S_2[\psi^\dagger,\psi] = -\pi\Gamma_2 \int d^dx \int \frac{d\omega}{2\pi}\frac{d\omega'}{2\pi}\frac{d\epsilon}{2\pi} \sum_{ij,\alpha\beta} \psi^\dagger_{i,\alpha}(x,\omega)\psi_{i,\alpha}(x,\omega+\epsilon)\sigma_3^{ij}\psi^\dagger_{j,\beta}(x,\omega'+\epsilon)\psi_{j,\beta}(x,\omega')$$

$$= -\pi\Gamma_2 \int d^dx \int \frac{d\omega}{2\pi}\frac{d\omega'}{2\pi}\frac{d\epsilon}{2\pi} \sum_{ij,\alpha\beta} \overline{\psi}_{i,\alpha}(x,\omega)\psi_{i,\alpha}(x,\omega+\epsilon)\sigma_3^{ij}\overline{\psi}_{j,\beta}(x,\omega'+\epsilon)\psi_{j,\beta}(x,\omega'). \tag{29}$$

Notice the following.

(1) Once again, the interaction does not mix the fields ψ in different thermal indices $i\neq j$; this is enforced by the σ_3 matrix in thermal space.

(2) The contributions from the two thermal components $i=1$ and 2 enter with opposite signs due to the negative sign for the time integration along the anti-time-ordered branch.

(3) Because all four fermions sit on the same index i, using the definition $\overline{\psi}_{j,\alpha}=\psi^\dagger_{i,\alpha}\sigma_3^{ij}$ does not change the structure of the interaction as the positive or negative signs from the σ_3 matrices always come in pairs.

We now introduce two Hubbard-Stratonovich fields X and Y to decouple the four fermion interactions.

$$e^{iS_1[\overline{\psi},\psi]} = \int DY\, e^{iS_{\rm y}[Y]} \exp\left(i\sqrt{2\pi\Gamma_1}\int d^dx \int \frac{d\omega}{2\pi}\frac{d\omega'}{2\pi} \sum_{ij,\alpha\beta} \overline{\psi}_{i,\alpha}(x,\omega)Y^{ij,\alpha\beta}_{\omega\omega'}(x)\psi_{j,\beta}(x,\omega') \right), \tag{30}$$

$$e^{iS_2[\overline{\psi},\psi]} = \int DX\, e^{iS_{\rm x}[X]} \exp\left(\sqrt{2\pi\Gamma_2}\int d^dx \int \frac{d\omega}{2\pi}\frac{d\omega'}{2\pi} \sum_{ij,\alpha\beta} \overline{\psi}_{i,\alpha}(x,\omega)X^{ij,\alpha\beta}_{\omega\omega'}(x)\psi_{j,\beta}(x,\omega') \right), \tag{31}$$

where

$$X^{ij,\alpha\beta}_{\omega\omega'} = \mathrm{X}^{i,\alpha\beta}(\omega-\omega')\,\delta_{ij}, \quad Y^{ij,\alpha\beta}_{\omega\omega'} = \mathrm{Y}^{i}(\omega-\omega')\,\delta_{\alpha\beta}\delta_{ij}.$$

Notice that the matrices $X^{ij,\alpha\beta}_{\omega\omega'}$ and $Y^{ij,\alpha\beta}_{\omega\omega'}$ depend only on the energy difference $\omega-\omega'$. We choose X Hermitian ($X=X^\dagger$), and Y to be anti-Hermitian ($Y=-Y^\dagger$); we could alternatively, have absorbed a factor of i into Y and made it Hermitian. The action for the matrices X and Y is

$$S_{\rm x}[X] = \frac{1}{2}\int d^dx \int \frac{d\epsilon}{2\pi}\mathrm{X}^{i,\alpha\beta}(\epsilon)\sigma_3^{ij}\mathrm{X}^{j,\beta\alpha}(-\epsilon), \tag{32}$$

$$S_{\rm y}[Y] = \frac{1}{2}\int d^dx \int \frac{d\epsilon}{2\pi}\mathrm{Y}^{i}(\epsilon)\sigma_3^{ij}\mathrm{Y}^{j}(-\epsilon). \tag{33}$$

The action for the $i=1$ and 2 components of X and Y in Eqs. (32) and (33) come with opposite signs, which is necessary to generate the correct sign in the four fermion terms for time-ordered and anti-time-ordered pieces. The fact that at

least one of the components is not positive definite is not a problem here because we work with a real time path integral and have the i factor in front of the actions S_x and S_y as in Eqs. (30) and (31).

Including the fields X and Y together with the matrix field Q, and integrating out the fermions, we can write the partition function (vacuum persistence) as

$$Z=\int DQ\,DX\,DY\,e^{(-1/2u)\int d^dx\,\mathrm{tr}\,Q^2}e^{iS_x[X]}e^{iS_y[Y]}\times\exp\left\{\int d^dx\,\mathrm{tr},\ln\left[-i\Omega-i\left(\frac{\nabla^2}{2m}+\epsilon_F\right)\mathbf{1}+\eta\Lambda+Q(x)-\sqrt{2\pi\Gamma_2}X(x)-i\sqrt{2\pi\Gamma_1}Y(x)\right]\right\}. \tag{34}$$

D. Expansion around the diffusive Fermi-liquid fixed point

We will now expand tr ln around the Q saddle of a diffusive Fermi liquid. The saddle-point solution for the noninteracting problem is $Q=\pi u\nu_0\Lambda$, where ν_0 is the density of states at the Fermi level and Λ is given in Eq. (27). The matrix Q can be rescaled so that the saddle point can be parametrized as $Q=U^\dagger\Lambda U$. The matrix Q in the nonlinear σ model then satisfies the constraints

$$Q=Q^\dagger,\quad Q^2=\mathbf{1},\quad \mathrm{tr}\,Q=0. \tag{35}$$

The expansion is achieved by allowing a slow position dependence in the matrix $U\to U(x)$, and considering small couplings $\Gamma_{1,2}$ and small energies ω. Expanding Eq. (34) around the saddle point, we have

$$Z=\int DX\,DY\,DQ\,e^{iS_x[X]}e^{iS_y[Y]}\exp\left(-\frac{1}{2}\int d^dx\{D\,\mathrm{tr}\,(\nabla Q)^2+4z\,\mathrm{tr}[(i\Omega-\eta\Lambda)Q]+2\sqrt{2\pi\Gamma_2}\ \mathrm{tr}\,(XQ)+2i\sqrt{2\pi\Gamma_1}\ \mathrm{tr}\,(YQ)\}\right), \tag{36}$$

where we have also absorbed the rescaling of the saddle into the couplings $\Gamma_{1,2}$, as well as D and z. Integrating out X and Y, we obtain $Z=\int DQ\,e^{-S[Q]}$, with an effective action for Q as follows:

$$S[Q]=S_D[Q]+S_{e\text{-}e}[Q],$$

where

$$S_D[Q]=\frac{1}{2}\int d^dx\{D\,\mathrm{tr}(\nabla Q)^2+4z\,\mathrm{tr}[(i\Omega-\eta\Lambda)Q]\}, \tag{37}$$

$$S_{e-e}[Q]=\int d^dx[i\pi\Gamma_1 Q\gamma_1 Q-i\pi\Gamma_2 Q\gamma_2 Q], \tag{38}$$

and the contractions $Q\gamma_1 Q$ and $Q\gamma_2 Q$ correspond to

$$Q\gamma_1 Q=\sum_{i,\alpha\beta}\int\frac{d\omega_1}{2\pi}\frac{d\omega_2}{2\pi}\frac{d\omega_3}{2\pi}\frac{d\omega_4}{2\pi}Q^{ii,\alpha\alpha}_{\omega_1\omega_2}Q^{ii,\beta\beta}_{\omega_3\omega_4}\sigma_3^{ii}\,2\pi\delta(\omega_1-\omega_2+\omega_3-\omega_4), \tag{39}$$

$$Q\gamma_2 Q=\sum_{i,\alpha\beta}\int\frac{d\omega_1}{2\pi}\frac{d\omega_2}{2\pi}\frac{d\omega_3}{2\pi}\frac{d\omega_4}{2\pi}Q^{ii,\alpha\beta}_{\omega_1\omega_2}Q^{ii,\beta\alpha}_{\omega_3\omega_4}\sigma_3^{ii}\,2\pi\delta(\omega_1-\omega_2+\omega_3-\omega_4). \tag{40}$$

At this stage we would like to compare the expressions for the effective nonlinear σ model [Eqs. (37) and (38)]. First, notice that the structure is very close to Finkelstein's replicated model; however, here we have only two ''replicas'' corresponding to the two thermal indices. Also, the interaction terms $Q\gamma_1 Q$ and $Q\gamma_2 Q$ do not couple the two thermal spaces much in the same way that the interaction does not couple different replicas. In the Schwinger-Keldysh approach the two thermal indices appear with an opposite sign; hence σ_3^{ii}, in contrast to δ_{ij}, as is the case of replicas.

IV. PARAMETRIZATION OF THE SADDLE

We have used above the parametrization $Q=U^\dagger\Lambda U$, where $\Lambda=\Sigma_{3\mathrm{Energy}}\otimes\sigma_{3\mathrm{Thermal}}\otimes\mathbf{1}_{\mathrm{Spin}}$. The tensor product of the Σ_3 in energy space and σ_3 in thermal space makes the parametrization of the saddle rather cumbersome for carrying out calculations. This can be resolved through the use of a transformation that allows us to parametrize around the saddle point

$$\tilde{\Lambda}^{ij,\alpha\beta}_{\omega\omega'}=\mathrm{sgn}\ \omega\,\delta_{\omega\omega'}\delta_{ij}\ \ \delta_{\alpha\beta}$$

$$\text{or}\ \ \tilde{\Lambda}=\underbrace{\Sigma_3}_{\text{Energy}}\otimes\underbrace{\mathbf{1}}_{\text{Thermal}}\otimes\underbrace{\mathbf{1}}_{\text{Spin}}.$$

In this case the thermal and spin structures for the saddle become trivial, and we need only to worry about the energy structure. This transformation is achieved through

$$Q\to T^\dagger QT,$$

where

$$T^{ij,\alpha\beta}_{\omega\omega'}=\begin{cases}\delta_{\omega,\omega'}\delta_{ij}\delta_{\alpha\beta}, & i=1\\ \delta_{\omega,-\omega'}\delta_{ij}\delta_{\alpha\beta}, & i=2.\end{cases}$$

The matrix T can be viewed as a direct product of matrices in energy, thermal and spin spaces: $T=U(i)\otimes\mathbf{1}_{\mathrm{thermal}}\otimes\mathbf{1}_{\mathrm{spin}}$, where $U(i)$ is a rotation in energy space that dependes on the thermal index. This transformation leaves the form of the action invariant, with the exception of $\Lambda\to\tilde{\Lambda}$ and $\Omega\to\tilde{\Omega}$, where

$$\tilde{\Omega}^{ij,\alpha\beta}_{\omega\omega'} = \omega \delta_{\omega\omega'} \sigma_3^{ij} \delta_{\alpha\beta}.$$

It is easy to check that the forms of $Q\gamma_1 Q$ and $Q\gamma_2 Q$ remain unchanged upon using the transformation T (the interaction does not mix thermal indices, so for $i=1$ this is trivial, and for $i=2$ one can absorb all changes in sign by redefining the integration variables).

The parametrization of Q around the $\tilde{\Lambda}$ saddle becomes simple and familiar, as in the work of Hikami:[31]

$$Q = \begin{bmatrix} \omega'>0 & \omega'<0 \\ \sqrt{1-V^\dagger V} & V^\dagger \\ V & -\sqrt{1-VV^\dagger} \end{bmatrix} \begin{matrix} \\ \omega>0 \\ \omega<0, \end{matrix} \tag{41}$$

where the matrix $V_{\omega\omega'}$ has row indices with negative energies ($\omega<0$) and column indices with positive energies ($\omega'>0$). As in several other works (see, for example, the work by McKane and Stone,[32] and by Grilli and Sorella[33]), we will proceed with the study of the nonlinear σ model by expanding in powers of the $V, V^\dagger$ matrices:

$$Q = \sum_n Q^{(n)},$$

where n is the order in the power series expansion in $V, V^\dagger$. For example,

$$Q^{(0)} = \begin{bmatrix} 1 & 0 \\ 0 & -1 \end{bmatrix}, \quad Q^{(1)} = \begin{bmatrix} 0 & V^\dagger \\ V & 0 \end{bmatrix},$$

$$Q(2) = -12\, V\dagger V 0012\, VV\dagger,$$

$$Q^{(3)} = 0, \quad Q^{(4)} = \begin{bmatrix} -\frac{1}{8}(V^\dagger V)^2 & 0 \\ 0 & \frac{1}{8}(VV^\dagger)^2 \end{bmatrix}, \quad \cdots.$$

The quadratic piece of the expansion of the action $S_D[Q]$ in powers of $V, V^\dagger$ is

$$S_D^{(2)}[Q] = \frac{1}{2}\int d^dx \{D \,\mathrm{tr}\,(\nabla Q^{(1)})^2 + 4z \,\mathrm{tr}[(i\tilde{\Omega} - \eta\tilde{\Lambda}) Q^{(2)}]\} \tag{42}$$

$$= \frac{1}{2}\int d^dx \int \frac{d\omega}{2\pi}\int \frac{d\omega'}{2\pi} \sum_{ij,\alpha\beta} [D\,\nabla Q^{(1)ij,\alpha\beta}_{\omega\omega'} \nabla Q^{(1)ji,\beta\alpha}_{\omega'\omega} + 4z(i\tilde{\Omega}^{ij,\alpha\beta}_{\omega\omega'} - \eta\tilde{\Lambda}^{ij,\alpha\beta}_{\omega\omega'}) Q^{(2)ji,\beta\alpha}_{\omega'\omega}] \tag{43}$$

$$= \int d^dk \int_{\omega>0} \frac{d\omega}{2\pi}\int_{\omega'<0} \frac{d\omega'}{2\pi} \sum_{ij,\alpha\beta} [Dk^2 - iz(\omega\sigma_3^{ii} - \omega'\sigma_3^{jj})] V^{\dagger ij,\alpha\beta}_{\omega\omega'}(k) V^{ji,\beta\alpha}_{\omega'\omega}(-k), \tag{44}$$

and

$$S_{e\text{-}e}^{(2)}[Q] = \int d^dx [i\pi\Gamma_1 Q^{(1)}\gamma_1 Q^{(1)} - i\pi\Gamma_2 Q^{(1)}\gamma_2 Q^{(1)}], \tag{45}$$

with

$$Q^{(1)}\gamma_1 Q^{(1)} = \sum_{i,\alpha\beta} \int \frac{d\omega_1}{2\pi}\frac{d\omega_2}{2\pi}\frac{d\omega_3}{2\pi}\frac{d\omega_4}{2\pi} Q^{(1)ii,\alpha\alpha}_{\omega_1\omega_2} Q^{(1)ii,\beta\beta}_{\omega_3\omega_4} \sigma_3^{ii} 2\pi\delta(\omega_1 - \omega_2 + \omega_3 - \omega_4) \tag{46}$$

$$= 2\sum_{i,\alpha\beta} \int_{\omega_1,\omega_4>0} \frac{d\omega_1}{2\pi}\frac{d\omega_4}{2\pi} \int_{\omega_2,\omega_3<0} \frac{d\omega_2}{2\pi}\frac{d\omega_3}{2\pi} V^{\dagger ii,\alpha\alpha}_{\omega_1\omega_2} V^{ii,\beta\beta}_{\omega_3\omega_4} \sigma_3^{ii} 2\pi\delta(\omega_1 - \omega_2 + \omega_3 - \omega_4), \tag{47}$$

$$Q^{(1)}\gamma_2 Q^{(1)} = \sum_{i,\alpha\beta} \frac{d\omega_1}{2\pi}\frac{d\omega_2}{2\pi}\frac{d\omega_3}{2\pi}\frac{d\omega_4}{2\pi} Q^{(1)ii,\alpha\beta}_{\omega_1\omega_2} Q^{(1)ii,\beta\alpha}_{\omega_3\omega_4} \sigma_3^{ii} 2\pi\delta(\omega_1 - \omega_2 + \omega_3 - \omega_4) \tag{48}$$

$$= 2\sum_{i,\alpha\beta} \int_{\omega_1,\omega_4>0} \frac{d\omega_1}{2\pi}\frac{d\omega_4}{2\pi} \int_{\omega_2,\omega_3<0} \frac{d\omega_2}{2\pi}\frac{d\omega_3}{2\pi} V^{\dagger ii,\alpha\beta}_{\omega_1\omega_2} V^{ii,\beta\alpha}_{\omega_3\omega_4} \sigma_3^{ii} 2\pi\delta(\omega_1 - \omega_2 + \omega_3 - \omega_4). \tag{49}$$

Notice that the contribution to quadratic order coming from $Q^{(2)}\gamma Q^{(0)}$ vanishes due to the trace, as do contributions to any order in the expansion of $Q\gamma Q$ where $Q^{(0)}$ appears as one of the two Q terms.

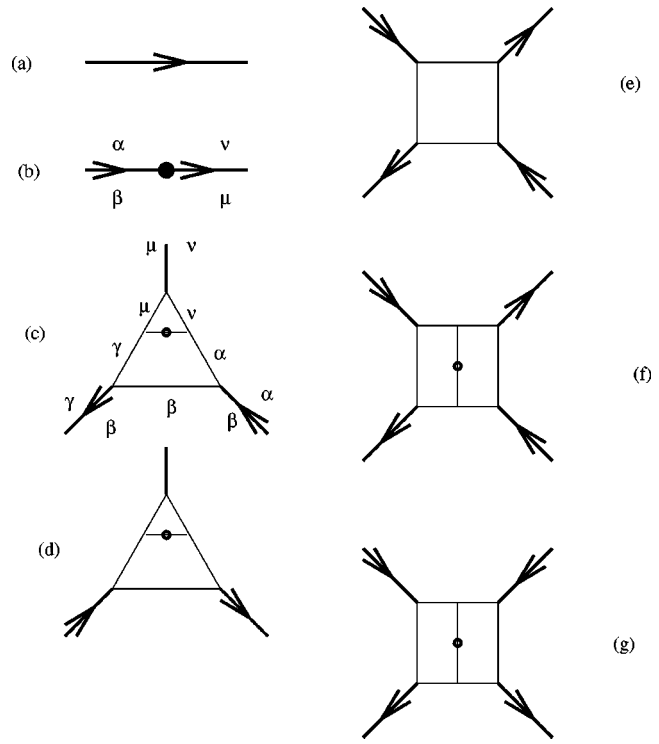

FIG. 3. The propagator and two-, three-, and four-point vertices.

V. FEYNMAN RULES

We now present the Feynman rules which follow from the action $S_D+S_{e\text{-}e}$. Our theory is parametrized most succinctly in terms of the V matrix used above. The basic propagator is the $\langle VV\rangle$ propagator or diffusion propagator which follows from S_D. It is represented by a thick line, as in Fig. 3(a), but it can be understood as a double line comprised of an electron and a hole. It carries momentum q and the two frequencies ϵ and $\epsilon+\omega$ of the electron and hole. The arrow is in the direction of the larger frequency. The propagator also carries two thermal indices and two spin indices (one each for the electron and the hole). The action $S_D+S_{e\text{-}e}$ contains terms of all orders in V. However, not all of these are needed at the one-loop level, as we now show.

Let us start by counting which vertices we need to include in the renormalization program. We can determine the loop order of any diagram[33,34] by considering the number n_ν of vertices with ν legs, and the number of external lines E. The number of legs in all vertices must equal the number of external legs plus twice the number of internal lines (each internal line belongs to two vertices):

$$E+2I=\sum_\nu \nu n_\nu . \tag{50}$$

The loop order is the net number of momentum integrals, which is the number of internal lines minus the number of contraints from momentum conservation in each vertex, plus an overall momentum conservation constraint

$$L=I-\sum_\nu n_\nu+1. \tag{51}$$

Thus

$$L=\sum_\nu n_\nu\left(\frac{1}{2}\nu-1\right)-\frac{1}{2}E+1. \tag{52}$$

With these relations in hand, it is simple to check that we only need to consider three and four point vertices in the one-loop ($L=1$) renormalization of the σ model. As mentioned above, the RG flows can be obtained from the two-point function alone, so we set $E=2$. Thus we have

$$1=\sum_\nu n_\nu\left(\frac{1}{2}\nu-1\right), \tag{53}$$

which has only two solutions: ($\nu=3, n_\nu=2$) or ($\nu=4, n_\nu=1$).

Hence, at the one-loop level, we need only consider the two-point vertex which follows from the expansion of $S_{e\text{-}e}$ to quadratic order in the V matrix; the triangle vertices which follow from its expansion to third order in V; and the square vertices which follow from its expansion to fourth order as well as the expansion of S_D to fourth order. The index structure of the former follows from Eq. (46). The index structure of the latter two follow from the fact that the thick lines are understood as splitting at the vertices to give the thin lines of the vertices; frequencies, spin, and thermal indices from the thick lines then split and follow the thin lines, as we demonstrate with the spin indices in Fig. 3(c). At the interaction dots, they follow the same rules as at the two-point vertices. In Fig. 3(b), there is a matrix structure $\delta^{\alpha\gamma}\delta^{\mu\nu}$ if the interaction dot is a Γ_1 and $\delta^{\alpha\mu}\delta^{\gamma\nu}$ if the interaction dot is a Γ_2. This is abbreviated as Γ. The frequencies have an overall δ-function at the dot. The Feynman rules are summarized below.

Propagator and diffusion vertex. At the one-loop level, we need only consider the first two terms in the expansion of S_D. They are the propagator and the diffusion vertex. The propagator is given by

$$\begin{aligned}(a)&=\langle V^{\dagger ij,\alpha\beta}_{\omega_1\omega_2}(q)V^{kl,\mu\nu}_{\omega_3\omega_4}(-q)\rangle\\&=\frac{1}{-iz(\omega_1\sigma_3^{ii}-\omega_2\sigma_3^{jj})+Dq^2}\,\delta^{il}\delta^{jk}\delta^{\alpha\nu}\delta^{\beta\mu}\\&\quad\times 2\pi\delta(\omega_1-\omega_4)2\pi\delta(\omega_2-\omega_3).\end{aligned} \tag{54}$$

The second term in the expansion of S_D is the box (e). It is given by

$$\begin{aligned}(e)&=\frac{D}{8}[2(q_1\cdot q_3+q_2\cdot q_4)+(q_1+q_3)\cdot(q_2+q_4)]\\&\quad+i\frac{z}{16}[\omega_1\sigma_3^{ii}-\omega_2\sigma_3^{jj}+\text{perm.}].\end{aligned} \tag{55}$$

We have omitted in the expression above the momentum and frequency conserving δ functions. The q_i's are the momenta on the four external legs. These legs can have arrows alternating between in and out as one goes around the box, with two pointing in and two pointing out.

Interaction vertices. The two-point vertex results from the lowest-order term in the expansion of $S_{e\text{-}e}$:

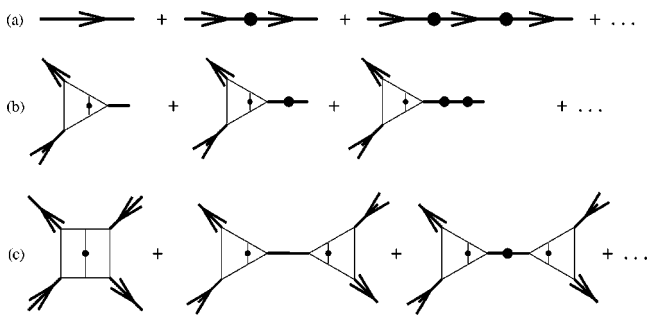

FIG. 4. The geometric series of diagrams which decorate the two-, three-, and four-point vertices.

$$(b)=2\pi i(-\Gamma_1\,\delta^{\alpha\beta}\delta^{\mu\nu}+\Gamma_2\delta^{\alpha\nu}\delta^{\beta\mu})\sigma_3^{ii}\times 2\pi\delta(\omega_1-\omega_2+\omega_3-\omega_4). \tag{56}$$

The next terms in the expansion of the interaction are the triangle terms:

$$(c),(d)=\mp i\pi\Gamma, \tag{57}$$

where Γ can be either Γ_1 or Γ_2 (the suppressed index structure is an extension of the two-point case, as we discussed above) and the arrowless propagator can have an arrow pointing in either direction.

Diagrams (f) (and a similar one with the arrows reversed) and (g) are the quartic terms resulting from the expansion of the interaction.

$$(f)=-i\pi\frac{\Gamma}{4},\quad (g)=+i\pi\frac{\Gamma}{2}. \tag{58}$$

Decoration of the interaction vertices. At the one-loop level, we do not need to consider terms of higher order than the above. However, there can still be terms of arbitrarily high order in Γ because there are quadratic interaction terms. These can be obtained by grouping all of the quadratic terms together and inverting them to obtain the full propagator:

$$\begin{aligned}\langle V^{\dagger ij,\alpha\beta}_{\omega_1\omega_2}(q)V^{kl,\mu\nu}_{\omega_3\omega_4}(-q)\rangle=&D_0\delta^{il}\delta^{jk}\delta^{\alpha\nu}\delta^{\beta\mu}2\pi\delta(\omega_1-\omega_4)2\pi\delta(\omega_2-\omega_3)\\&-2\pi i\Gamma_1D_1D_2\delta^{ij}\delta^{il}\delta^{jk}\delta^{\alpha\beta}\delta^{\mu\nu}2\pi\delta(\omega_1-\omega_2+\omega_3-\omega_4)\\&+2\pi i\Gamma_2D_2D_0\delta^{ij}\delta^{il}\delta^{jk}\delta^{\alpha\nu}\delta^{\beta\mu}2\pi\delta(\omega_1-\omega_2+\omega_3-\omega_4).\end{aligned} \tag{59}$$

Note that the interaction terms are distinguished from the propagator by the δ^{ij} on the thermal indices and the overall δ energy function. Here $z_1=z-2\Gamma_1+\Gamma_2\equiv z-2\Gamma_s$ and $z_2=z+\Gamma_2\equiv z-2\Gamma_t$, where we have introduced the singlet and triplet interaction amplitudes, $\Gamma_s=\Gamma_1-\Gamma_2/2$, $\Gamma_t=-\Gamma_2/2$ by rewriting

$$\Gamma_1\delta^{\alpha\beta}\delta^{\mu\nu}-\Gamma_2\delta^{\alpha\nu}\delta^{\beta\mu}=\left(\Gamma_1-\frac{1}{2}\Gamma_2\right)\delta^{\alpha\beta}\delta^{\mu\nu}-\frac{1}{2}\Gamma_2\sigma^{\alpha\beta}\sigma^{\mu\nu}. \tag{60}$$

The inversion is more simply done in the singlet-triplet decomposition since these matrices are orthogonal. It can then be reexpressed in Eq. (59), where D_0, D_1, and D_2 are given by

$$D_0=\frac{1}{-iz(\omega_1\sigma_3^{ii}-\omega_2\sigma_3^{jj})+Dq^2},$$

$$D_1=\frac{1}{-iz_1(\omega_1\sigma_3^{ii}-\omega_2\sigma_3^{jj})+Dq^2}, \tag{61}$$

$$D_2=\frac{1}{-iz_2(\omega_1\sigma_3^{ii}-\omega_2\sigma_3^{jj})+Dq^2}.$$

Hence, by inverting the sum of all of the quadratic terms (rather than just the quadratic term coming from S_D) and amputating the propagators entering and leaving the vertex, we effect the replacement

$$(b)=2\pi i\left(-\Gamma_1\frac{D_1D_2}{D_0^2}\delta^{\alpha\beta}\delta^{\mu\nu}+\Gamma_2\frac{D_2}{D_0}\delta^{\alpha\nu}\delta^{\beta\mu}\right)\sigma_3^{ii}\times 2\pi\delta(\omega_1-\omega_2+\omega_3-\omega_4). \tag{62}$$

This can, equivalently, be obtained by summing the geometric series of Fig. 4(a). It is this peculiar property of this theory — namely that there are quadratic interactions — which lead to one-loop RG equations which have terms of all orders in Γ_2.

Similarly, when the interaction in (c), (d), (f), or (g) is on an internal line, we can sum the infinite series of Figs. 4(b) or 4(c) and, again, make the replacements

$$\Gamma_1\to\Gamma_1\frac{D_1D_2}{D_0^2},\quad \Gamma_2\to\Gamma_2\frac{D_2}{D_0}. \tag{63}$$

While the decoration of vertices leads to a replacement of propagators (63), the decoration of propagators themselves — and, in particular, external legs — is superfluous since the first term in Eq. (59), which has the desired index structure, is not affected by decoration. The decoration of an external line of a vertex amounts to propagator decoration and is similarly ignored.

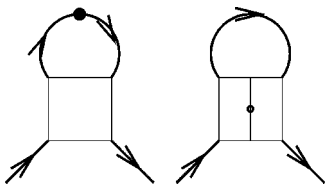

FIG. 5. The self-energy diagrams which renormalize z and D.

VI. RENORMALIZATION OF THE σ MODEL

There are four couplings, $D, z, \Gamma_{1,2}$, in our action,

$$S=\frac{1}{2}\int d^2x\{D\,\mathrm{tr}\,(\nabla Q^{(1)})^2+\mathrm{tr}[(4iz\tilde{\Omega}-\eta\tilde{\Lambda})Q^{(2)}]\}$$
$$+\int d^dx[i\pi\Gamma_1 Q^{(1)}\gamma_1 Q^{(1)}-i\pi\Gamma_2 Q^{(1)}\gamma_2 Q^{(1)}]. \tag{64}$$

All of these couplings are present in the quadratic terms in the action. Hence the RG flows can be computed from the two-point function alone, separating the different contributions according to their spin, frequency, and Schwinger-Keldysh matrix structures.

First, there is the diffusion constant, D — or, equivalently, the resistivity, $g=1/[(2\pi)^2 D]$. In the noninteracting σ model, this is the only coupling constant. In the interacting case, it is still used as the expansion parameter: we assume that g is small, but make no assumptions about $\Gamma_{1,2}$. The second coupling constant is z, the relative rescaling of time versus space. g and z are renormalized by the diagrams of Fig. 5. The other couplings are the interactions $\Gamma_{1,2}$, which are renormalized by the diagrams of Figs. 6–13. Contributions to the Q self-energy determine the flow of D or z if they are proportional to q^2 or ω, respectively, provided they have the correct thermal index structure. They determine the flow of $\Gamma_{1,2}$ if they are independent of the external and frequency and are diagonal in the thermal indices; they contribute to one or the other depending on their spin structure.

It is a matter of taste whether or not we choose to introduce a ''wave-function'' renormalization ζ (the quotation marks refer to the fact that we mean a renormalization of V, not ψ), since this can be completely absorbed in the renormalization of D and z. There is a natural definition of ζ which is related to the density of states, but this is moot for the scaling equations which we consider because we can rescale our couplings to eliminate ζ. Hence, we sweep the wave-function renormalization under the rug in this paper.

At tree level, D, z, and $\Gamma_{1,2}$ are marginal. [One might have expected $\Gamma_{1,2}$ to have the dimensions of $(\mathrm{length})^{-2}$, but they do not as a result of the extra frequency integral]. To find the fluctuation corrections to their scaling behavior, we use a

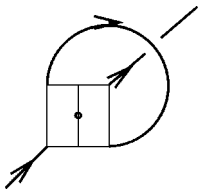

FIG. 6. The lowest-order diagram which renormalizes $\Gamma_{1,2}$.

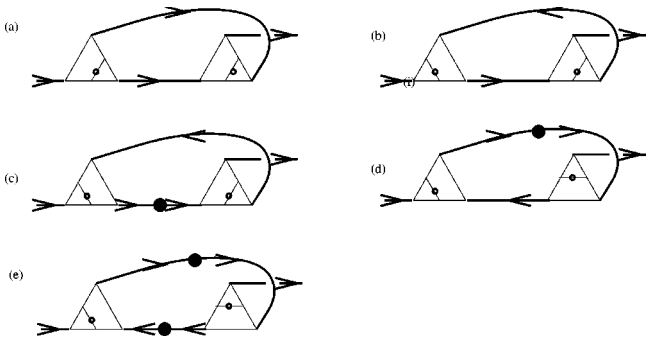

FIG. 7. The five ''primitive'' diagrams which renormalize Γ_1. They are elaborated in Figs. 8–10. The corresponding elaboration for Γ_2 is in Figs. 11–13.

Wilsonian shell elimination scheme in which we compute their change as we integrate out shells

$$\Lambda-d\Lambda<Dq^2<\Lambda,\quad 0<\omega<\Lambda$$

and

$$\Lambda-d\Lambda<\omega<\Lambda,\quad 0<Dq^2<\Lambda. \tag{65}$$

Renormalization of D and z. Let us examine Fig. 5. By inspection, we see that these diagrams have the appropriate matrix structure for the propagator, i.e., the matrix structure of Eq. (54). Diagrams without an interaction vertex do not contribute to the renormalization of D to one-loop order; the reason for this is that there is a cancellation between the two (time-ordered and anti-time-ordered) Schwinger-Keldysh species. In the case of the replica calculation, the contribution to one-loop order is proportional to the replica number $N\to 0$.

The diagrams in Fig. 5 give the following contribution to the Q-field self-energy Σ:

$$\Sigma(q,\Omega+\epsilon,\epsilon)=\Sigma_A(q,\Omega+\epsilon,\epsilon)+\Sigma_B(q,\Omega+\epsilon,\epsilon), \tag{66}$$

where

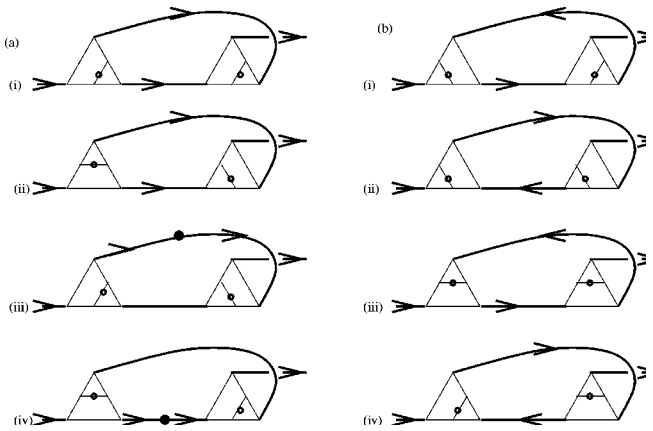

FIG. 8. Diagrams (a) and (b) renormalizing Γ_1.

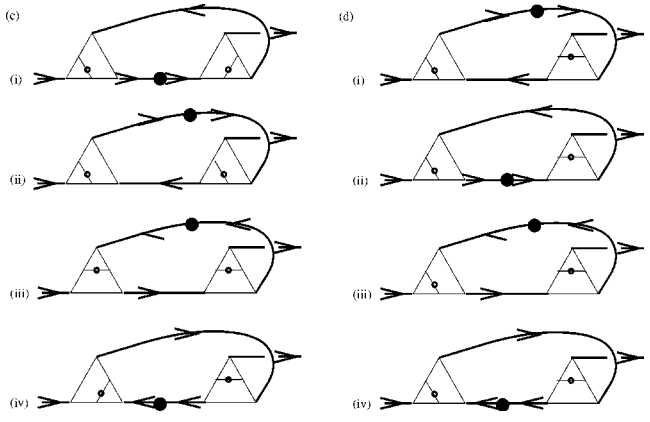

FIG. 9. Diagrams (c) and (d) renormalizing Γ_1.

$$\Sigma_A(q,\Omega+\epsilon,\epsilon) = -4\int \frac{d^2k}{(2\pi)^2}\frac{d\omega}{2\pi}(-2\pi i) \times[\Gamma_1(k,\omega)-2\Gamma_2(k,\omega)]D_0^2(k,\omega) \times\left[\frac{D}{8}(k+q)^2 - i\frac{z}{8}(\omega+\Omega)\right] \tag{67}$$

is the contribution of the diagram on the left, and

$$\Sigma_B(q,\Omega+\epsilon,\epsilon) = 4\int \frac{d^2k}{(2\pi)^2}\frac{d\omega}{2\pi}\left(-\frac{\pi i}{4}\right)[\Gamma_1(k-q,\omega-\Omega) -2\Gamma_2(k-q,\omega-\Omega)]D_0(k,\omega) \tag{68}$$

is the contribution of the diagram on the right. There is a relative factor of 2 between the Γ_1 and Γ_2 contributions because the former contribution has no free internal spin indices, while the latter has one which is summed over. Notice that Σ_A and Σ_B cancel at $q=\Omega=0$. The contribution of Σ_A as well as a piece of Σ_B are absorbed into the wave-function renormalization. The Σ_B contribution includes a term of the form

$$4\Gamma_2\int \frac{d^2k}{(2\pi)^2}\frac{d\omega}{2\pi}D_0(k,\omega)D_2(k,\omega), \tag{69}$$

which comes from differentiating D_0 with respect to q^2. The wave-function renormalization multiplies the V fields, and therefore resurfaces in the renormalization of Γ_2. Differentiating with respect to ω or q^2, respectively, we get, to lowest order in $\Gamma_{1,2}$, the one-loop contributions to dD and dz (the external frequencies and momenta have been set to zero after differentiation):

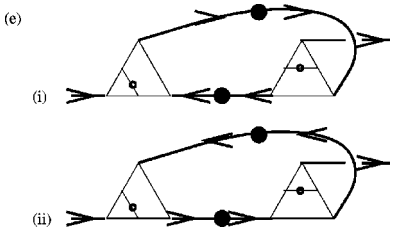

FIG. 10. Diagrams (e) renormalizing Γ_1.

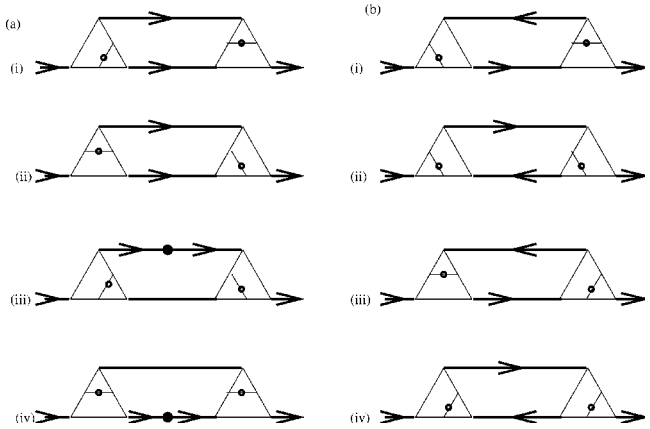

FIG. 11. Diagrams (a) and (b) renormalizing Γ_2.

$$dD = -\left(\frac{d\Sigma_B}{dq^2}\right)_{q=0,\Omega=0} = -D(-2\pi i)\int \frac{d^2k}{(2\pi)^2}\frac{d\omega}{2\pi} \times[\Gamma_1(k,\omega)-2\Gamma_2(k,\omega)]D_0^3(k,\omega)Dk^2, \tag{70}$$

$$dz = -i\left(\frac{d\Sigma_B}{d\Omega}\right)_{q=0,\Omega=0} = -\frac{1}{2}\int \frac{d^2k}{(2\pi)^2}[\Gamma_1(k,0)-2\Gamma_2(k,0)]D_0(k,0). \tag{71}$$

In the dz term, the Ω derivative cancels the ω integral.

Making the replacement (63), we obtain

$$-\frac{dD}{D} = (-2\pi i)\int \frac{d^2k}{(2\pi)^2}\frac{d\omega}{2\pi}Dk^2[\Gamma_1 D_0(k,\omega) \times D_1(k,\omega)D_2(k,\omega) - 2\Gamma_2 D_0^2(k,\omega)D_2(k,\omega)], \tag{72}$$

$$dz = -\frac{1}{2}(\Gamma_1-2\Gamma_2)\int \frac{d^2k}{(2\pi)^2}D_0(k,0). \tag{73}$$

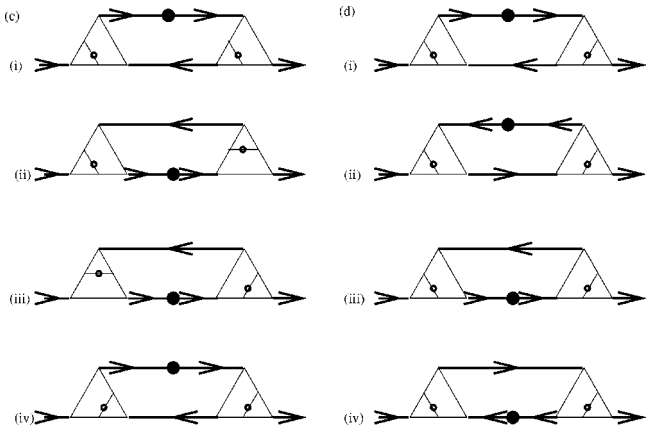

FIG. 12. Diagrams (c) and (d) renormalizing Γ_2.

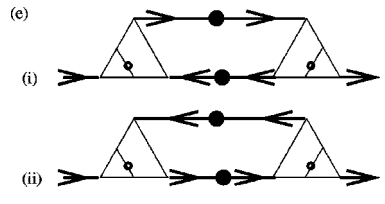

FIG. 13. Diagrams (e) renormalizing Γ_2.

The contribution to dz is unchanged but the contribution to dD receives corrections of all order in $\Gamma_{1,2}$. This result is the full one-loop result: it is lowest order in g but to all orders in $\Gamma_{1,2}$.

Integrals (70) and (72) are discussed in the appendixes. Here we just state the results:

$$\frac{dg}{dl}=g^2[\Gamma_1 f_2(z,z_1,z_2)-2\Gamma_2 f_2(z,z,z_2)],$$

$$\frac{dz}{dl}=g(-\Gamma_1+2\Gamma_2), \tag{74}$$

where $dl=-d(\ln\Lambda)$ and we have made the substitution $g=1/8\pi D$.[35] Following Finkelstein, we have introduced the functions

$$f_1(z,z_2)=\frac{1}{z_2-z}\ln\left(\frac{z_2}{z}\right),$$

$$f_2(z,z_1,z_2)=\frac{2z_1}{z_1-z_2}f_1(z,z_1)-\frac{2z_2}{z_1-z_2}f_1(z,z_2). \tag{75}$$

As we show in the appendixes, the functions $f_{1,2}$ arise as a result of the mismatch between the poles of the propagators $D_{0,1,2}$. In the noninteracting case, in which these propagators are equal, these functions are just constants, $f_1(z,z)=1, f_2(z,z,z)=2$. Interactions split the energies of singlet and triplet particle-hole states from their noninteracting value, leading to Eq. (75).

Renormalization of $\Gamma_{1,2}$. The diagrams which renormalize Γ_1 are in Figs. 6 and 8–10, while the related diagrams which renormalize Γ_2 are in Figs. 6 and 8–10. In Figs. 8–13, we have, for the sake of completeness and pedagogy, enumerated all of the diagrams which contribute to the renormalization of $\Gamma_{1,2}$. On combinatoric grounds, we see that we have included all 20 of the diagrams which contribute to Γ_1, and the 20 which contribute to Γ_2. All of these diagrams must be taken into account to obtain the correct signs and relative coefficents of various terms in the RG equations. However, these two sets of 20 are really elaborations of two sets of five diagrams. In Fig. 7, we give the five basic diagrams for Γ_1; Figs. 8–13 are put in Appendix A to avoid unnecessary clutter and confusion. From Fig. 7(a) we obtain the six diagrams of Fig. 8(a). From each of Figs. 7(b), 7(c), and 7(d), we obtain four diagrams shown, respectively, in Figs. 8(b), 9(c), and 9(d). Finally, Fig. 7(e) gives rise to the two diagrams of Fig. 10.

In Fig. 6, Γ_1 contributes to the renormalization of Γ_2, and vice versa. When only Γ_2's appear in Figs. 8–13, the spin index structures dictate that Figs. 8–10 contribute to the flow of Γ_1 while Figs. 11–13 contribute to the flow of Γ_2. If any of the vertices are Γ_1's, however, corresponding diagrams in Figs. 8–10 and 11–13 cancel. Hence, we need only consider Γ_2's in Figs. 7–13.

By following the frequencies and spin indices around the diagram of Fig. 6, we see that it gives a contribution

$$d\Gamma_1\delta^{\alpha\beta}\delta^{\mu\nu}-d\Gamma_2\delta^{\alpha\nu}\delta^{\beta\mu}$$
$$=(\Gamma_1\delta^{\alpha\nu}\delta^{\beta\mu}-\Gamma_2\delta^{\alpha\beta}\delta^{\mu\nu})\int\frac{d^2k}{(2\pi)^2}D_0(k,\omega). \tag{76}$$

Corresponding diagrams of Figs. 8–10 and 11–13 give identical contributions, apart from a factor of 2 coming from a spin sum, so we will focus on Figs. 8–10. Figure 8(a) gives a contribution

$$-2\pi i\,d\Gamma_1=(i\pi\Gamma_2)^2\int\frac{d^2k}{(2\pi)^2}\frac{d\omega}{2\pi}D_0^2(k,\omega). \tag{77}$$

The signs of the six diagrams [(iii) and (iv) are two diagrams each because the arrow can point in either direction on the arrowless lines] are determined by the relative signs of the two triangle vertices (57). The first two diagrams come with a positive sign while the other four come with a negative sign. Adding these together, we obtain the coefficient -2. Both of the interaction ''dots'' are on internal lines, so we make the replacement (63):

$$-2\pi i\,d\Gamma_1^{(a)}=-2(i\pi\Gamma_2)^2\int\frac{d^2k}{(2\pi)^2}\frac{d\omega}{2\pi}D_2^2(k,\omega). \tag{78}$$

In Fig. 8(b), there are four diagrams and they all come with positive signs. Only one interaction dot is on an internal line, so we have

$$-2\pi i\,d\Gamma_1^{(b)}=4(i\pi\Gamma_2)^2\int\frac{d^2k}{(2\pi)^2}\frac{d\omega}{2\pi}D_0(k,\omega)D_2(k,\omega). \tag{79}$$

The diagrams of Fig. 11(b) vanish because the integrated frequency is overdetermined. However, the wave-function renormalization coming from the neglected part of Σ_B makes up the missing contribution.

In Fig. 9(c), the four diagrams have positive signs. There are three interactions, but one is on an external line, so there is a contribution:

$$-2\pi i\,d\Gamma_1^{(c)}=4(i\pi\Gamma_2)^2(i2\pi\Gamma_2)$$
$$\times\int\frac{d^2k}{(2\pi)^2}\int_0^\Lambda\frac{d\omega_1}{2\pi}\int_{-\Lambda}^0\frac{d\omega_2}{2\pi}D_0(k,\omega_1-\omega_2)$$
$$\times[D_2(k,\omega_1-\omega_2)]^2$$
$$=4(i\pi\Gamma_2)^2(i2\pi\Gamma_2)$$
$$\times\int\frac{d^2k}{(2\pi)^2}\int_0^\Lambda\frac{d\omega}{2\pi}\frac{\omega}{2\pi}D_0(k,\omega)[D_2(k,\omega)]^2, \tag{80}$$

where we have set $\omega=\omega_1-\omega_2$ as the only variable inside the propagators, and obtained the phase-space factor $\omega/2\pi$ from integrating the intermediate frequencies.

Figure 9(d), on the other hand, comes with a negative sign and only one internal interaction:

$$-2\pi i\, d\Gamma_1^{(d)} = -4(i\pi\Gamma_2)^2(i2\pi\Gamma_2) \times \int \frac{d^2k}{(2\pi)^2}\int_0^\Lambda \frac{d\omega}{2\pi}\frac{\omega}{2\pi}[D_0(k,\omega)]^2 D_2(k,\omega). \tag{81}$$

The coefficient 4 is important for the physics of this theory. In Finkelstein's original paper,[5] the contributions from the diagrams of Fig. 9 were too small by a factor of 2. As a result, a metallic fixed point with infinite conductivity was found. This error was corrected in Refs. 36 and 37.

Finally, we have the two diagrams of Fig. 10(e):

$$-2\pi i\, d\Gamma_1^{(e)} = -2(i\pi\Gamma_2)^2(i2\pi\Gamma_2)^2 \times \int \frac{d^2k}{(2\pi)^2}\frac{d\omega}{2\pi}\left(\frac{\omega}{2\pi}\right)^2 \times [D_0(k,\omega)]^2[D_2(k,\omega)]^2, \tag{82}$$

where, as in Figs. 10(c) and 10(d), there are intermediate frequency integrals that lead to the phase-space factor $(\omega/2\pi)^2$.

The integrals in the expressions above are discussed in the appendixes. Their upshots are

$$\begin{aligned} d\Gamma_1^{(a)} &= -\frac{\Gamma_2^2}{z_2} g d(\ln\Lambda), \\ d\Gamma_1^{(b)} &= 2\Gamma_2^2 f_1(z,z_2) g d(\ln\Lambda), \\ d\Gamma_1^{(c)} &= -\frac{\Gamma_2^3}{z_2} f_2(z,z,z_2) g d(\ln\Lambda), \\ d\Gamma_1^{(d)} &= \frac{\Gamma_2^3}{z} f_2(z_2,z_2,z) g d(\ln\Lambda), \\ d\Gamma_1^{(e)} &= -\Gamma_2^4\left(\frac{\frac{1}{z}+\frac{1}{z_2}-2f_1(z,z_2)}{(z-z_2)^2}\right) g d(\ln\Lambda). \end{aligned} \tag{83}$$

Adding these contributions, we obtain

$$d\Gamma_1^{(a)}+d\Gamma_1^{(b)}+d\Gamma_1^{(c)}+d\Gamma_1^{(d)}+d\Gamma_1^{(e)} \equiv -\Phi = \frac{\Gamma_2^2}{z} g d(\ln\Lambda). \tag{84}$$

VII. RENORMALIZATION-GROUP EQUATIONS

Gathering these results, we have the flow equations

$$\begin{aligned} \frac{dg}{dl} &= g^2[\Gamma_1 f_2(z,z_1,z_2) - 2\Gamma_2 f_2(z,z,z_2)], \\ \frac{dz}{dl} &= g(-\Gamma_1+2\Gamma_2), \quad \frac{d\Gamma_1}{dl} = g\left(\Gamma_2+\frac{\Gamma_2^2}{z}\right), \\ \frac{d\Gamma_2}{dl} &= g\left(\Gamma_1+\frac{2\Gamma_2^2}{z}\right). \end{aligned} \tag{85}$$

Adding the second and fourth equations, and subtracting the third equation twice, we find

$$\frac{d}{dl}(z-2\Gamma_1+\Gamma_2)=0. \tag{86}$$

Although we have only verified Eq. (86) to one loop, it is, in fact, an exact relation which follows from the Ward identity for charge conservation, as we discuss in Appendix C.

Since a constant of integration in (86) can be absorbed into a rescaling of frequencies, we can set $\Gamma_1=(z+\Gamma_2)/2$. Changing variables from Γ_2 to $\gamma_2=\Gamma_2/z$ we have the equations

$$\begin{aligned} \frac{dg}{dl} &= g^2\left[1+3\left(1-\frac{1+\gamma_2}{\gamma_2}\ln(1+\gamma_2)\right)\right], \\ \frac{dz}{dl} &= zg\left(-\frac{1}{2}+\frac{3}{2}\gamma_2\right), \quad \frac{d\gamma_2}{dl} = \frac{g}{2}(1+\gamma_2)^2. \end{aligned} \tag{87}$$

From the final equation, we see that γ_2 increases at long length scales. This is not problematic since we made no assumptions about the smallness of Γ_2. When γ_2 becomes sufficiently large, z begins to grow, and g, after an initial increase, begins to decrease. Since these equations are valid in the small-g regime, it would appear that the flow improves their validity. However, γ_2 and z diverge at a finite length scale. Since these equations include all orders in γ_2, their breakdown signals the onset of nonperturbative physics.

It is useful, as a comparison, to consider the BCS interaction in a Fermi liquid. There the flow equation for the BCS interaction V can be computed to all orders in perturbation theory:

$$\frac{dV}{dl} = -V^2. \tag{88}$$

The one-loop RG result is the full story because there is only a geometric series of bubble diagrams. This equation also breaks down at a finite length scale — the coherence length. At this length scale, the nonperturbative physics of pairing takes over. Similarly, the breakdown of our flow equations (85) implies that nonperturbative physics—such as the formation of local moments — determines the behavior of the system. Such physics cannot be accessed perturbatively from the diffusive saddle point.

VIII. DISCUSSION

In this paper we have shown how the Schwinger-Keldysh dynamical formulation[26] can be applied in treating a disordered interacting electronic problem. We reproduce Finkelstein's renormalization-group equations for the interaction strength and conductance. In our approach, the RG procedure is carried out in a very simple way, in close resem-

blance to a ϕ^4 theory (with cubic terms as well).

For the case of the diffusive Fermi-liquid state, the calculation using the Schwinger-Keldysh method is very similar to the replica method. The two thermal indices for time-ordered and anti-time-ordered propagation play a similar role to that of the replica indices in the particular case of the diffusive Fermi-liquid regime studied by Finkelstein. The disorder couples fields with different thermal indices (or replicas), while the interaction does not mix thermal indices (or replicas). The Schwinger-Keldysh indices, like the replicas, act in this example as simple bookkeeping devices. In the replica calculation, the diffusive Fermi-liquid state is replica symmetric. This is the underlying physical reason for the simplicity of the replica structure.

There should exist much more interesting saddle points where the replica symmetry is broken. One such point is the Wigner glass phase, which occurs in the limit of low electronic densities. As in the cases with other types of glasses, such as spin glasses, we know that replica symmetry breaking is connected to broken ergodicity. In the Schwinger-Keldysh approach we expect that broken ergodicity (and thus replica symmmetry breaking) will manifest itself in subtleties related to the $\omega \to 0$ limit and the symmetry between time-ordered and anti-time-ordered products. The Schwinger-Keldysh provides a natural tool to study dynamical effects, which is a direction that we will explore.

ACKNOWLEDGMENTS

We would like to thank Sudip Chakravarty, Eduardo Fradkin, Patrick Lee, Adrianus M.M. Pruisken, and Michael Stone for discussions. The authors would like to thank the Institute for Theoretical Physics, UCSB, for hospitality during the workshops on Low-Dimensional Quantum Field Theory (1997) — where this work was begun — and Disorder and Interactions in the Quantum Hall Effect and Mesoscopic Systems (1998) — where this work was completed. This work was supported in part by the NSF under Grants Nos. NSF-PHY 94-07194 and NSF-DMR-94-24511 at the University of Illinois (C.C.), and by the A.P. Sloan Foundation (A.W.W.L.).

APPENDIX A: ELABORATION OF THE FIVE BASIC DIAGRAMS

The five basic diagrams of Fig. 7 are a schematic representation of the 20 diagrams in Figs. 8 and 9 which renormalize Γ_1. The corresponding diagrams which renormalize Γ_2 are shown in Figs. 11–13.

APPENDIX B: INTEGRALS

The following five logarithmically divergent integrals arise in the calculation of the diagram of Fig. 6 and diagrams (a)–(e) in Figs. 11–13. We define $x = Dq^2$ and integrate over the shells $\Lambda - d\Lambda < x < \Lambda, 0 < \omega < \Lambda$ and $\Lambda - d\Lambda < \omega < \Lambda, 0 < x < \Lambda$.

In the diagram of Fig. 4, there are no free frequencies; there is only a momentum integration

$$\frac{1}{4\pi D}\int dx\, D_0(x,\omega) = \frac{1}{4\pi D}\int_{\Lambda - d\Lambda}^{\Lambda} dx \frac{1}{x} = \frac{1}{4\pi D} d(\ln \Lambda). \tag{B1}$$

In diagrams (a)–(e) of Figs. 11–13, there are multiple propagators with different z's. By rewriting these products of propagators as a sum over poles in x and ω, we reduce them to $d(\ln\Lambda)$ times nondivergent integrals. These integrals give nontrivial functions of the z_i's.

$$\begin{aligned}
\frac{1}{2(2\pi)^2 D}\int dx\, d\omega\, D_0(x,\omega) D_2(x,\omega) &= \frac{1}{2(2\pi)^2 D}\int_{\Lambda - d\Lambda}^{\Lambda} dx \int_0^{\Lambda} d\omega \frac{1}{x - iz\omega}\frac{1}{x - iz_2\omega} \\
&\quad + \frac{1}{2(2\pi)^2 D}\int_{\Lambda - d\Lambda}^{\Lambda} d\omega \int_0^{\Lambda} dx \frac{1}{x - iz\omega}\frac{1}{x - iz_2\omega} \\
&= \frac{1}{2(2\pi)^2 D} d\Lambda \int_0^{\Lambda} d\omega \frac{i}{(z_2 - z)\omega}\left(\frac{1}{\Lambda - iz\omega} - \frac{1}{\Lambda - iz_2\omega}\right) \\
&\quad + \frac{1}{2(2\pi)^2 D}\frac{i}{(z_2 - z)}\frac{d\Lambda}{\Lambda}\int_0^{\Lambda} dx \left(\frac{1}{x - iz\Lambda} - \frac{1}{x - iz_2\Lambda}\right) \\
&= \frac{i}{z_2 - z}\ln\left(\frac{z_2}{z}\right)\frac{1}{2(2\pi)^2 D}\, d(\ln\Lambda) = i f_1(z, z_2)\frac{1}{2(2\pi)^2 D} d(\ln\Lambda).
\end{aligned} \tag{B2}$$

Similarly,

$$\frac{1}{2(2\pi)^2 D}\int dx\, d\omega\, x\, D_0(x,\omega)D_2(x,\omega)\, D_1(x,\omega)=\frac{1}{2(2\pi)^2 D}\int_{\Lambda-d\Lambda}^{\Lambda}dx\int_0^{\Lambda}d\omega\, x\frac{1}{x-iz\omega}\frac{1}{x-iz_2\omega}\frac{1}{x-iz_1\omega}$$
$$+\frac{1}{2(2\pi)^2 D}\int_{\Lambda-d\Lambda}^{\Lambda}d\omega\int_0^{\Lambda}dx\, x\frac{1}{x-iz\omega}\frac{1}{x-iz_2\omega}\frac{1}{x-iz_1\omega}$$
$$=\left[\frac{2iz_1}{(z_1-z_2)(z-z_1)}\ln\left(\frac{z}{z_1}\right)-\frac{2iz_2}{(z_1-z_2)(z-z_2)}\ln\left(\frac{z}{z_2}\right)\right]\frac{1}{2(2\pi)^2 D}d(\ln\Lambda)$$
$$=if_2(z,z_1,z_2)\frac{1}{2(2\pi)^2 D}d(\ln\Lambda), \tag{B3}$$

$$\frac{1}{2(2\pi)^2 D}\int dx\, d\omega\int_0^{\omega}d\omega'\, D_0(x,\omega)D_2(x,\omega)D_2(x,\omega)=\frac{1}{2(2\pi)^2 D}\int_{\Lambda-d\Lambda}^{\Lambda}dx\int_0^{\Lambda}\omega\, d\omega\frac{1}{x-iz\omega}\frac{1}{x-iz_2\omega}\frac{1}{x-iz_2\omega}$$
$$+\frac{1}{2(2\pi)^2 D}\int_{\Lambda-d\Lambda}^{\Lambda}\omega\, d\omega\int_0^{\Lambda}dx\frac{1}{x-iz\omega}\frac{1}{x-iz_2\omega}\frac{1}{x-iz_2\omega}$$
$$=-\frac{1}{2z_2}\left[\frac{2}{(z-z_2)}-\frac{2z_2}{(z-z_2)^2}\ln\left(\frac{z}{z_2}\right)\right]\frac{1}{2(2\pi)^2 D}d(\ln\Lambda)$$
$$=-\frac{1}{2z_2}f_2(z,z,z_2)\frac{1}{2(2\pi)^2 D}d(\ln\Lambda), \tag{B4}$$

$$\frac{1}{2(2\pi)^2 D}\int dx\, d\omega\, \omega^2\, D_0(x,\omega)D_0(x,\omega)D_2(x,\omega)\, D_2(x,\omega)$$
$$=\frac{1}{2(2\pi)^2 D}\int_{\Lambda-d\Lambda}^{\Lambda}dx\int_0^{\Lambda}\omega^2\, d\omega\frac{1}{x-iz\omega}\frac{1}{x-iz\omega}\frac{1}{x-iz_2\omega}\frac{1}{x-iz_2\omega}$$
$$+\frac{1}{2(2\pi)^2 D}\int_{\Lambda-d\Lambda}^{\Lambda}\omega^2\, d\omega\int_0^{\Lambda}dx\frac{1}{x-iz\omega}\frac{1}{x-iz\omega}\frac{1}{x-iz_2\omega}\frac{1}{x-iz_2\omega}$$
$$=-i\left(\frac{\frac{1}{z}+\frac{1}{z_2}-2f_1(z,z_2)}{(z-z_2)^2}\right)\frac{1}{2(2\pi)^2 D}d(\ln\Lambda). \tag{B5}$$

APPENDIX C: WARD IDENTITY

In Sec. VI, we found that our one-loop RG equations imply that

$$\frac{d}{dl}z=2\frac{d}{dl}\Gamma_s. \tag{C1}$$

We would now like to indicate why this constraint follows from charge conservation. Let us imagine returning to our disorder-averaged action $S_0+S_{\rm rand}+S_{\rm int}$ for interacting electrons. Let us consider some fixed realization of the disorder. The Ward identity which follows from charge conservation,

$$\partial_\mu\langle T[j_\mu(y)\psi^\dagger(x_1)\psi(x_2)]\rangle$$
$$=i\delta(y-x_1)\langle T[\psi^\dagger(x_1)\psi(x_2)]\rangle$$
$$-i\delta(y-x_2)\langle T[\psi^\dagger(x_1)\psi(x_2)]\rangle, \tag{C2}$$

relates vertex renormalization (the left-hand side) to the renormalization of the propagator (the right-hand side). This is more transparent in momentum space:

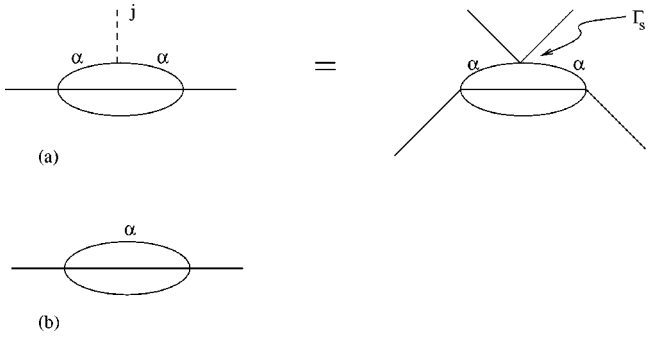

FIG. 14. Diagrams contributing to the renormalization of (a) Γ_s and (b) z.

$$\Lambda_\mu(p,0)=\frac{\partial}{\partial p_\mu}[\omega-\epsilon_p-\Sigma(p)]. \tag{C3}$$

$\Lambda_\mu(p,0)$ is the Fourier transform of the correlation function with a current insertion (at zero momentum) on the left-hand-side of (C2). Σ is the self-energy. We focus on the $\mu=0$ component of this equation:

$$\Lambda_0(p,0)=\frac{\partial}{\partial \omega}[\omega-\Sigma(p)]. \tag{C4}$$

The equality between the left- and right-hand sides is exemplified by the relation between the diagrams of Figs. 14(a) [the dashed line indicates the current insertion in the correlation function of the left-hand side of Eq. (C2)] and 14(b).

As we indicate in Fig. 14(a), the diagrams contributing tothe renormalization of the left-hand side of Eq. (C4) are equivalent to those which determine the RG flow of Γ_s.

Meanwhile, the diagrams contributing to the renormalization of the right-hand side of Eq. (C4) renormalize z. One way of seeing this is to note that the renormalization of the propagator determines the RG flow of z, since the former is the renormalization of the term $i\omega\psi^\dagger\psi$ in S_0 while the latter is the renormalization of the equivalent term in S_D, namely, $\mathrm{tr}[\omega Q]$. The factor of 2 on the right-hand side results from the summation over the spin index α in Fig. 14(b). This index is held fixed as an external index in the Γ_s renormalization.

In principle, we can derive the same result for disorder-averaged correlation functions directly within the σ model by deriving the corresponding Ward identity. However, this is more cumbersome because the current operator, and the gauge transformation rules are more complicated in the Q-field language.

[1] P.W. Anderson, Phys. Rev. **109**, 1492 (1958).
[2] D.J. Thouless, Phys. Rep. **13**, 93 (1974).
[3] F.J. Wegner, Z. Phys. B **35**, 207 (1979).
[4] E. Abrahams, P.W. Anderson, D.C. Licciardello, and T.V. Ramakrishnan, Phys. Rev. Lett. **42**, 673 (1979).
[5] A.M. Finkelstein, Zh. Éksp. Teor. Fiz. **84**, 168 (1983) [Sov. Phys. JETP **57**, 97 (1983)].
[6] C. Castellani, C. Di Castro, P.A. Lee, and M. Ma, Phys. Rev. B **57**, R9381 (1984).
[7] D. Belitz and T.R. Kirkpatrick, Rev. Mod. Phys. **66**, 261 (1994).
[8] A.M.M. Pruisken, M.A. Baranov, and B. Škorić, cond-mat/9712322,9712323 (unpublished); cond-mat/9712323 (unpublished).
[9] S.V. Kravchenko *et al.*, Phys. Rev. B **51**, 7038 (1995); Phys. Rev. Lett. **77**, 4938 (1996); D. Simonian, S.V. Kravchenko, M.P. Sarachik, and V.M. Pudalov, *ibid.* **79**, 2304 (1997).
[10] D. Popović, A.B. Fowler, and S. Washburn, Phys. Rev. Lett. **79**, 1543 (1997).
[11] Y. Hanien *et al.*, Phys. Rev. Lett. **80**, 1288 (1998); M.Y. Simmons *et al.*, *ibid.* **80**, 1292 (1998); S.J. Papadakis and M. Shayegan, Phys. Rev. B **57**, R15 068 (1998).
[12] J. Lam *et al.*, Phys. Rev. B **56**, R12 741 (1997); P.T. Coleridge *et al.*, *ibid.* **56**, R12 764 (1997).
[13] S. Chakravarty, S. Kivelson, C. Nayak, and K. Voelker, cond-mat/9805383 (unpublished).
[14] For a review, see T. Giamarchi and P. Le Doussal, in *Spin Glasses and Random Fields*, edited by A.P. Young (World Scientific, Singapore, 1997), and references therein.
[15] J. Schwinger, J. Math. Phys. **2**, 407 (1961).
[16] L.V. Keldysh, Zh. Éksp. Teor. Fiz. **47**, 1515 (1964) [Sov. Phys. JETP **20**, 1018 (1965)].
[17] J. Rammmer and H. Smith, Rev. Mod. Phys. **58**, 323 (1986).
[18] R.P. Feynman and F.L. Vernon, Jr., Ann. Phys. (N.Y.) **24**, 118 (1963).
[19] P.C. Martin, E. Siggia, and H.A. Rose, Phys. Rev. A **8**, 423 (1973); H.K. Janssen, Z. Phys. B **23**, 377 (1976); *Dynamics of Critical Phenomena and Related Topics*, edited by C.P. Enz, Lecture Notes in Physics Vol. 104 (Springer-Verlag, Berlin, 1979).
[20] H. Sompolinsky, Phys. Rev. Lett. **47**, 935 (1981); H. Sompolinsky and A. Zippelius, Phys. Rev. B **25**, 6860 (1982).
[21] H.G. Schuster and V.R. Vieira, Phys. Rev. B **34**, 189 (1986).
[22] R. Kree, Z. Phys. B **65**, 505 (1987).
[23] M.L. Horbach and G. Schön, Ann. Phys. (Leipzig) **2**, 51 (1993).
[24] L.F. Cugliandolo and G. Lozano, cond-mat/9807138.
[25] A.V. Andreev and A. Kamenev, preceding paper, Phys. Rev. B **60**, 2218 (1999).
[26] C. Chamon, A.W.W. Ludwig, and C. Nayak (unpublished).
[27] G.W. Semenoff and H. Umezawa, Nucl. Phys. B **220**, 196 (1983).
[28] A.J. Niemi and G.W. Semenoff, Ann. Phys. (N.Y.) **152**, 105 (1984); Nucl. Phys. B **230**, 181 (1984).
[29] N. P. Landsman and Ch. G. van Weert, Phys. Rep. **145**, 141 (1987).
[30] $Z^{C_3\cup C_4}$ contains the statistical information such as $F=-T\ln Z^{C_3\cup C_4}$, which is not our main interest here. For this reason we ignore it.
[31] S. Hikami, Phys. Rev. B **24**, 2671 (1981).
[32] A.J. McKane and M. Stone, Ann. Phys. (N.Y.) **131**, 36 (1981).
[33] M. Grilli and S. Sorella, Nucl. Phys. B **295**, 422 (1988).
[34] E. Brézin, J.C. Le Guillou, and J. Zinn-Justin, in *Phase Transitions and Critical Phenomena*, edited by C. Domb and M.S. Green (Academic Press, London, 1976), Vol. 6.
[35] By rescaling our Q field to set $Q^2=1$, and absorbing the resulting factor of the density of states ν_0 into Γ_1, we have essentially set $\nu_0=2/\pi$. Consequently, our conductance is slightly different from the conventional $g=1/(2\pi)^2 D$.
[36] C. Castellani, C. Di Castro, P.A. Lee, M. Ma, S. Sorella, and E. Tabet, Phys. Rev. B **30**, 1596 (1984).
[37] A.M. Finkelstein, Z. Phys. B **56**, 189 (1984).